JACS
JOURNAL OF THE AMERICAN CHEMICAL SOCIETY

Subscriber access provided by American Chemical Society

Article

Electronic Configuration Assignment and the Importance of Low-Lying Excited States in High-Spin Imidazole-Ligated Iron(II) Porphyrinates

Chuanjiang Hu, Arne Roth, Mary K. Ellison, Jin An,
Christina M. Ellis, Charles E. Schulz, and W. Robert Scheidt

J. Am. Chem. Soc., **2005**, 127 (15), 5675-5688• DOI: 10.1021/ja044077p • Publication Date (Web): 25 March 2005

Downloaded from http://pubs.acs.org on March 25, 2009

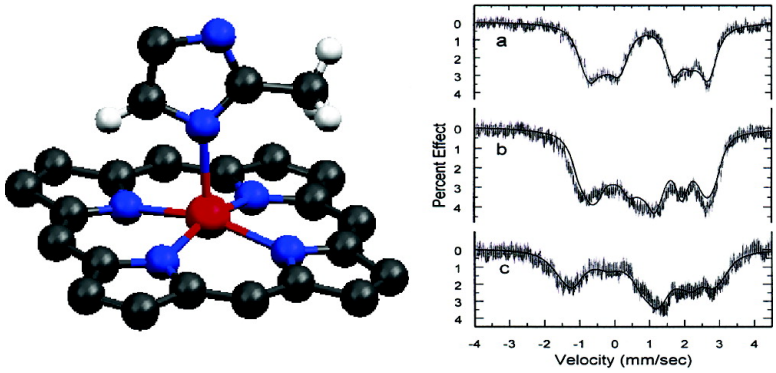

More About This Article

Additional resources and features associated with this article are available within the HTML version:

- Supporting Information
- Links to the 7 articles that cite this article, as of the time of this article download
- Access to high resolution figures
- Links to articles and content related to this article
- Copyright permission to reproduce figures and/or text from this article

View the Full Text HTML

ACS Publications
High quality. High impact.

Journal of the American Chemical Society is published by the American Chemical Society. 1155 Sixteenth Street N.W., Washington, DC 20036

J|A|C|S
ARTICLES
Published on Web 03/25/2005

Electronic Configuration Assignment and the Importance of Low-Lying Excited States in High-Spin Imidazole-Ligated Iron(II) Porphyrinates

Chuanjiang Hu,[†] Arne Roth,[†] Mary K. Ellison,[†] Jin An,[†] Christina M. Ellis,[‡] Charles E. Schulz,*[,‡] and W. Robert Scheidt*[,†]

Contribution from the Department of Chemistry and Biochemistry, University of Notre Dame, Notre Dame, Indiana 46556, and Department of Physics, Knox College, Galesburg, Illinois 61401

Received September 28, 2004; E-mail: scheidt.1@nd.edu

Abstract: The synthesis and characterization of six new high-spin deoxymyoglobin models (imidazole-(tetraarylporphyrinato)iron(II)) are described. These have been intensively studied by temperature-dependent Mössbauer spectroscopy from 295 to 4.2 K. All complexes show a strong temperature dependence for the quadrupole splitting consistent with low-lying excited states of the same or lower multiplicity. An analysis of the data obtained in applied magnetic fields leads to the assignment of the sign of the quadrupole splitting. All model compounds as well as those of deoxymyoglobin and deoxyhemoglobin, previously studied, have a negative sign for the quadrupole splitting. Although not previously predicted, this experimental observation leads to the assignment of the ground-state electronic configuration for all high-spin *imidazole-ligated* iron(II) porphyrinates as $(d_{xz})^2(d_{yz})^1(d_{xy})^1(d_{z^2})^1(d_{x^2-y^2})^1$. This is a distinctly different ground-state electronic configuration from other high-spin iron(II) porphyrinates; differences in structural details for the two classes of high-spin complexes are also discussed. The apparent anomaly of differing signs for the zero-field splitting constant between previously studied model complexes and the heme proteins is addressed; the difference appears to result from the fact that the assumptions used in the spin Hamiltonian approach that has been applied to these complexes are not adequately satisfied. Structures of four of the new five-coordinate species have been determined. Core conformations in these derivatives show variation, but these and previously studied compounds reveal a limited number of conformational patterns. The bond lengths and other geometrical parameters such as porphyrin core size and iron out-of-plane displacement support a high-spin state assignment for the iron(II).

Introduction

Iron porphyrinate complexes (hemes) are the active sites in many biologically important systems. Knowledge of both the electronic and geometric structure at iron appears to be the key to understanding the many diverse and complicated functions of these hemoproteins. Indeed, the electronic ground states of models of these iron(II) species have been intensively investigated both experimentally and theoretically and yet are far from being determined with certainty.

One widely spread class of heme-based systems are those that bind the diatomic molecules O_2, NO, or CO. The primary purposes of binding diatomic molecules include transport, storage and sensing. Sensing proteins include the FixL system,[1] which detects the presence of O_2, and the guanylate cyclase system,[2] which detects NO and functions in the control of blood pressure. The best known systems are the O_2-binding proteins myoglobin and hemoglobin, which shuttle between deoxy- and oxy-states. The iron of the hemes remains in the 2+ formal oxidation state. In the deoxy state, the iron(II) is five-coordinate and bound to the protein by the proximal histidine ligand. The hemes become six-coordinate upon binding of an O_2 molecule.

In an early—dare we say heroic—study, Pauling and Coryell[3] measured the magnetic moments for a number of hemoprotein systems including deoxyhemoglobin and oxyhemglobin. The oxy state is found to be diamagnetic, whereas the deoxy state is high spin with four unpaired electrons.[3a] The structural changes that accompany the spin state change are essential to the mechanism of cooperative O_2-binding by hemoglobin and are the basis of the T → R transition of hemoglobin.[4−6] In brief, the five-coordinate deoxy heme has a structure with a significant displacement of the iron atom out of the heme plane whereas the six-coordinate oxyheme has the iron in the plane. The

[†] University of Notre Dame.
[‡] Knox College.

(1) (a) Rodgers, K. R.; Lukat-Rodgers, G. S.; Barron, J. A. *Biochemistry* **1996**, *35*, 9539. (b) Miyatake, H.; Mukai, M.; Park, S. Y.; Adachi, S.; Tamura, K.; Nakamura, H.; Tsuchiya, T.; Lizuka, T.; Shiro, Y. *J. Mol. Biol.* **2000**, *301*, 415.
(2) (a) Murad, F. *J. Clin. Invest.* **1986**, *78*, 1. (b) Waldman, S. A.; Murad, F. *Pharmacol. Rev.* **1987**, *39*, 163.
(3) (a) Pauling, L.; Coryell, C. D. *Proc. Natl. Acad. Sci. U.S.A.* **1936**, *22*, 159. (b) Pauling, L.; Coryell, C. D. *Proc. Natl. Acad. Sci. U.S.A.* **1936**, *22*, 211. (c) Coryell, C. D.; Stitt, F.; Pauling, L. *J. Am. Chem. Soc.* **1937**, *59*, 633.
(4) Perutz, M. F. *Nature* **1970**, *228*, 226.
(5) Perutz, M. F. *Nature* **1972**, *237*, 495.
(6) Perutz, M. F.; Fermi, G.; Luisi, B.; Shaanan, B.; Liddington, R. C. *Acc. Chem. Res.* **1987**, *20*, 309.

signaling of the binding state between the four hemes of tetrameric hemoglobin as dioxygen is bound forms the basis of the cooperativity and is strongly coupled to the structure of the five-coordinate iron(II) porphyrin sites.

The structural features of the five-coordinate heme considered to be of prime functional significance are the out-of-plane displacement of the iron with respect to the porphyrin plane, the porphyrin core conformation, which is usually considered to have features in accord with C_{4v} doming, the axial bond distance, and possible changes in orientation and off-axis tilts of the proximal imidazole ligand. Despite these interesting and important features, relatively little structural information is available on five-coordinate imidazole-ligated iron(II) species. There are two practical reasons: (i) the compounds are easily oxidized to iron(III) complexes, and (ii) the equilibrium of binding only one imidazole to an iron(II) porphyrinate is quite unfavorable. Thus, the synthesis of six-coordinate bis-ligated complexes is much easier than that of five-coordinate species.

A synthetic strategy for preparing five-coordinate imidazole-ligated high-spin iron(II) derivatives was reported by Reed and Collman in 1973[7] and used the sterically hindered 2-methylimidazole ligand. This ligand is expected to lead to a significantly distorted molecule only if a six-coordinate species was formed. However, stereochemical issues concerning five-coordinate species remain. The crystalline complex of [Fe(TPP)(2-MeHIm)][8] prepared by Reed and Collman was structurally characterized in the laboratory of the late Prof. J. L. Hoard. A preliminary report of the structure was given at an American Chemical Society meeting,[9] and results were additionally cited and used by Hoard and Scheidt,[10] but complete structural details were never published. One crystallographic feature that marred the metrical usefulness of the structure was the presence of crystallographically required two-fold disorder normal to the porphyrin plane. This two-fold axis leads to positional disorder in the axial imidazole and significantly limits the accuracy of some features involving the axial ligand and possibly that of the porphyrin ligand as well. A related species, [Fe(TpivPP)(2-MeHIm)], also displayed this type of disorder[11] and suffers the same limitations. We recently reported the structure of a new, more ordered variant of the five-coordinate species [Fe(TPP)(2-MeHIm)]. As noted below this new structure reveals a number of stereochemically important features for iron(II) porphyrinates that are possibly functionally significant.[12]

Quite surprisingly, the two crystalline forms of [Fe(TPP)(2-MeHIm)] show both geometric and electronic structure differences. Although the two structures show many common features that are expected for high-spin iron(II) species (large iron atom displacement, long $Fe-N_p$ bonds), there are also some interesting differences. The earlier [Fe(TPP)(2-MeHIm)] structure[9] has a domed core with a substantial out-of-plane displacement of the iron[13] whereas the later structure[12] had a much less domed core with a smaller out-of-plane displacement of the iron. Indeed, the core conformation showed a stepped (or wave) conformation with an apparent asymmetry in the equatorial bonds related to the orientation of the axial imidazole ligand. As part of a more general program of characterization of high-spin iron(II) porphyrinates, we have now determined the molecular structure of four new high-spin imidazole-ligated iron(II) porphyrinates to determine if there are general structural features for this class of derivative.

We have also been concerned with the electronic structure of this class of heme species, which can be considered to be model compounds for deoxymyoglobin and deoxyhemoglobin. The electronic structure of iron(II) hemes is quite challenging to study since most spectroscopic probes provide little or no information about the states of the d^6 metal ion. Iron(II) is a non-Kramers system and, except in fortuitous circumstances is EPR silent. Fortunately, Mössbauer spectroscopy has proven to be an extremely useful spectroscopic probe for the electronic structure of iron(II), and we report detailed results in applied magnetic field for all new derivatives. The Mössbauer data measured for the four new high-spin iron(II) samples in both zero and applied magnetic field, along with previously studied porphyrin derivatives, provide a consistent picture of the electronic structure. Imidazole-ligated iron(II) porphyrinates form a distinctly different set of electronic structures than iron(II) porphyrinates with other axial ligands.

The difficulty of understanding the electronic structure of the five-coordinate imidazole-ligated hemes is reflected in both the relatively large amount published on the issue and some changing interpretations for both experimental and theoretical studies. A number of recent density functional theory (DFT) studies for five-coordinate imidazole-ligated hemes have appeared.[14−17] However, the conclusions reached about the electronic ground state are by no means uniform. Three of the four DFT calculations found that a triplet state was lower in energy than the experimentally observed quintet state. In all of these cases, a quintet state is predicted to be lowest in energy when the iron(II) atom is constrained to be further out of the porphyrin plane than the value obtained for the triplet state. In other words, DFT says large values of ΔFe stabilize higher spin multiplicities. The fourth study[16] does predict a quintet ground state.

A key issue for completely defining the quintet state of the imidazole-ligated model compounds can be simply stated as "which of the five occupied d-orbitals is the doubly populated orbital?" The possibilities include (i) $(d_{xz})^1(d_{yz})^1(d_{xy})^2(d_{z^2})^1(d_{x^2-y^2})^1$, (ii) $(d_{xz})^1(d_{yz})^1(d_{xy})^1(d_{z^2})^2(d_{x^2-y^2})^1$, (iii) $(d_{xz})^2(d_{yz})^1(d_{xy})^1(d_{z^2})^1(d_{x^2-y^2})^1$,

(7) Collman, J. P.; Reed, C. A. *J. Am. Chem. Soc.* **1973**, *95*, 2048.
(8) The following abbreviations are used in this paper: Porph, a generalized porphyrin dianion; T*p*-OCH_3PP, dianion of *meso*-tetra-*p*-methoxyphenylporphyrin; TPP, dianion of *meso*-tetraphenylporphyrin; TTP, dianion of *meso*-tetratolylporphyrin, TpivPP, dianion of α,α,α,α-tetrakis(*o*-pivalamidophenyl)porphyrin; Piv_2C_8P, dianion of α,α,5,15-[2,2′-(octanediamido)diphenyl]-α,α,10−20-bis(o-pivalamidophenyl)porphyrin; Im, generalized imidazole; RIm, generalized hindered imidazole; HIm, imidazole; 1-MeIm, 1-methylimidazole; 2-MeHIm, 2-methylimidazole; 1,2-Me_2Im, 1,2-dimethylimidazole; N_p, porphyrinato nitrogen; Ct, the center of four porphyrinato nitrogen atoms; EPR, electron paramagnetic resonance; NRVS, nuclear resonance vibrational spectroscopy.
(9) (a) Collman, J. P.; Kim, N.; Hoard, J. L.; Lang, G.; Radonovich, L. J.; Reed, C. A. *Abstracts of Papers*; 167th National Meeting of the American Chemical Society; Los Angeles, CA, April 1974; American Chemical Society: Washington, DC, 1974; INOR 29. (b) Hoard, J. L., personal communication to WRS. In particular, Prof. Hoard provided a set of atomic coordinates for the molecule.
(10) Hoard, J. L.; Scheidt, W. R. *Proc. Natl. Acad. Sci. U.S.A.* **1973**, *70*, 3919.
(11) Jameson, G. B.; Molinaro, F. S.; Ibers, J. A.; Collman, J. P.; Brauman, J. I.; Rose, E.; Suslick, K. S. *J. Am. Chem. Soc.* **1980**, *102*, 3224.
(12) Ellison, M. K.; Schulz, C. E.; Scheidt, W. R. *Inorg. Chem.* **2002**, *41*, 2173.
(13) One convenient measure of core doming is given by the difference in the displacement of the iron from the mean plane of four nitrogen atoms compared to the displacement from the from the 24-atom mean plane.
(14) Rovira, C.; Kunc, K.; Hutter, J.; Ballone, P.; Parrinello, M. *J. Phys. Chem. A* **1997**, *101*, 8914.
(15) Kozlowski, P. M.; Spiro, T. G.; Zgierski, M. Z. *J. Phys. Chem. B* **2000**, *104*, 10659.
(16) Liao, M.-S.; Scheiner, S. *J. Chem. Phys.* **2002**, *116*, 3635.
(17) Ugalde, J. M.; Dunietz, B.; Dreuw, A.; Head-Gordon, M.; Boyd, R. J. *J. Phys. Chem. A* **2004**, *108*, 4653.

or (iv) $(d_{xz})^1(d_{yz})^2(d_{xy})^1(d_{z^2})^1(d_{x^2-y^2})^1$. The latter two states are nominally degenerate but may differ in energy, owing to the relative orientation of the axial imidazole ligand with respect to the porphyrin core. The DFT calculations fail to provide a clear picture to this question. The experimental Mössbauer data, however, clearly rule out some orbital population possibilities and suggests a clear, most probable electronic configuration. Moreover, an examination of all Mössbauer data for high-spin iron(II) with a wide variety of axial ligands suggests the division of high-spin iron(II) porphyrinates into two classes of electronic configuration.

Finally, we examine the issues of the differing crystal field parameters that have been reported for the proteins deoxymyoglobin and -hemoglobin and the imidazole-ligated iron(II) porphyrinates, the interpretation of which has changed significantly over time. The crystal field analyses are based on the most recent Mössbauer[12,18] and magnetic susceptibility studies.[19−21] A distinct difference, seemingly unexpected, is that the proteins and the models show differing signs of the zero-field splitting parameter, *D*, and the rhombicity *E*/*D* of the crystal field among the studied compounds. A synopsis of the analyses for imidazole-ligated iron(II) porphyrinates derivatives is that all of the model complexes analyzed to date[12,18,22] have negative zero-field splitting constants, while the heme proteins myoglobin and hemoglobin[18] have *positive* values of the zero-field splitting constant. While most of the assignments are based on Mössbauer spectroscopy, the pattern of differing signs is also supported by an integer spin EPR study.[23]

Since the difference in the sign of *D* requires major differences in the relative orbital energies of the d_{xz}, d_{yz}, and d_{xy} orbitals, as described in the Discussion, achieving an understanding of the origin of the apparent difference between the proteins and the model complexes was desirable. We have used Mössbauer spectroscopy in applied magnetic field to determine the sign of the zero-field splitting constant for several new high-spin imidazole-ligated iron porphyrinates. While a completely satisfactory solution to the understanding of the question of the differences in the sign of *D* has not been found, further insight and a path for additional study has been accomplished.

The analysis in this contribution allows us to give the best experimental electronic configuration to date for all known imidazole-ligated high-spin iron(II) porphyrinates: $(d_{xz})^2(d_{yz})^1(d_{xy})^1(d_{z^2})^1(d_{x^2-y^2})^1$. This assignment is equally valid for the analogous heme proteins. Moreover, in hemes, this electronic configuration appears to be found only for high-spin imidazole-ligated iron(II) species; all other high-spin five-coordinate iron(II) derivatives have a different electronic configuration.

Experimental Section

General Information. All reactions and manipulations for the preparation of the iron(II) porphyrin derivatives (see below), were carried out under argon using a double-manifold vacuum line, Schlenkware and cannula techniques. Benzene and hexanes were distilled over sodium benzophenone ketyl. Ethanethiol (Aldrich) was used as received. Chlorobenzene was purified by washing with concentrated sulfuric acid, then with water until the aqueous layer was neutral, then dried with $MgSO_4$, and then distilled twice over P_2O_5. 2-Methylimidazole and 1,2-dimethylimidazole were purchased from Aldrich, recrystallized from toluene, and dried under vacuum. The free-base porphyrin ligands *meso*-tetra-*p*-methoxyphenylporphyrin (H_2T*p*-OCH_3PP), *meso*-tetratolylporphyrin (H_2TTP), and *meso*-tetraphenylporphyrin (H_2TPP) were prepared according to Adler et al.[24] The metalations of the free-base porphyrins to give [Fe(Porph)Cl] were done as previously described.[25] [Fe(T*p*-OCH_3PP)]$_2$O, [Fe(TTP)]$_2$O, and [Fe(TPP)]$_2$O were prepared according to a modified Fleischer preparation.[26]

The following reactions were carried out under strict anaerobic conditions. All solvents were degassed prior to use by three freeze/pump/thaw cycles. The four-coordinate species [Fe(II)(T*p*-OCH_3PP)] was prepared by reduction of [Fe(T*p*-OCH_3PP)]$_2$O (0.04 mmol) in benzene (10 mL) with excess ethanethiol (1.0 mL, >200-fold) according to Stolzenberg et al.[27] The benzene solution was stirred overnight followed by solvent removal under vacuum. [Fe(II)(TTP)] was prepared from [Fe(TTP)]$_2$O as above. [Fe(II)(TPP)] was prepared from [Fe(TPP)]$_2$O as above, except that toluene was used as the solvent. Solid [Fe(II)(Porph)] samples were never exposed to air to avoid the easily formed [Fe(Porph)]$_2$O. UV−vis spectra were recorded on a Perkin-Elmer Lambda 19 UV/vis/near-IR spectrometer, and IR spectra were recorded on a Perkin-Elmer Paragon 10000 or Nicolet Nexus 670 FT-IR spectrometer as KBr pellets. Mössbauer measurements were performed on a constant acceleration spectrometer from 4.2 to 300 K with optional small field and in a 9-T superconducting magnet system (Knox College). Samples for Mössbauer spectroscopy were prepared by immobilization of the crystalline material in Apiezon M grease.

Synthesis of [Fe(T*p*-OCH_3PP)(2-MeHIm)] and [Fe(T*p*-OCH_3PP)(1,2-Me_2Im)]. The complexes were prepared by dissolving the precipitated [Fe(T*p*-OCH_3PP)] (0.08 mmol) in chlorobenzene, adding ~1 mL ethanethiol by pipet and a C_6H_5Cl solution of imidazole (2-fold excess) by cannula. The reaction mixture was then stirred for 24 h. UV−vis in C_6H_5Cl: λ_{max}, nm; for [Fe(T*p*-OCH_3PP)(2-MeHIm)], 370, 438, 540, 571, 612; for [Fe(T*p*-OCH_3PP)(1,2-Me_2Im)], 371, 439, 541, 568, 613.

Synthesis of [Fe(TPP)(1,2-Me_2Im)]. In this case, after reduction with ethanethiol, the toluene was not removed under vacuum, but a toluene solution of 1,2-dimethylimidazole (2-fold excess) was added by cannula directly to the solution of [Fe(TPP)] (0.08 mmol). UV−vis in C_6H_5Cl: λ_{max}, nm; 369, 435, 538, 563, 608.

Synthesis of [Fe(TTP)(2-MeHIm)]. This complex was prepared by adding excess ligands (2-methylimidazole) (0.4 mmol) in chlorobenzene (15 mL) by cannula to the solid [Fe(II)(TTP)] and stirred for 1 h. UV−vis in C_6H_5Cl: λ_{max}, nm; 368, 439, 538, 567, 613.

For all imidazole complexes, X-ray quality crystals were obtained in 8 mm × 250 mm sealed glass tubes by liquid diffusion using hexanes as non-solvent after 10 days (in the case of [Fe(TPP)(1,2-Me_2Im)] and [Fe(TTP)(2-MeHIm)]) and three weeks (in the case of [Fe(T*p*-OCH_3-PP)(2-MeHIm)] and [Fe(T*p*-OCH_3PP)(1,2-Me_2Im)]). Microcrystalline solids for Mössbauer measurements were obtained by liquid diffusion in Schlenk tubes using hexanes as the nonsolvent. The solids were isolated in an inert-atmosphere box and immobilized in Nylon sample holders.

X-ray Structure Determinations. Single-crystal experiments were carried out on a Bruker Apex system with graphite monochromated Mo K radiation ($\lambda = 0.71073$ Å). The crystalline samples were placed

(18) Kent, T. A.; Spartalian, K.; Lang, G. *J. Chem. Phys.* **1979**, *71*, 4899.
(19) Nakano, N.; Otsuka, J.; Tasaki, A. *Biochim. Biophys. Acta* **1971**, *236*, 222.
(20) Nakano, N.; Otsuka, J.; Tasaki, A. *Biochim. Biophys. Acta* **1972**, *278*, 355.
(21) Alpert, A.; Banerjee, R. *Biochim. Biophys. Acta* **1975**, *405*, 114.
(22) Kent, T. A.; Spartalian, K.; Lang, G.; Yonetani, T.; Reed, C. A.; Collman, J. P. *Biochim. Biophys. Acta* **1979**, *580*, 245.
(23) Hendrich, M. P.; Debrunner P. G. *J. Magn. Reson.* **1988**, *78*, 133−141.
(24) Adler, A. D.; Longo, F. R.; Finarelli, J. D.; Goldmacher, J.; Assour, J.; Korsakoff, L. *J. Org. Chem.* **1967**, *32*, 476.
(25) (a) Adler, A. D.; Longo, F. R.; Kampus, F.; Kim, J. *J. Inorg. Nucl. Chem.* **1970**, *32*, 2443. (b) Buchler, J. W. In *Porphyrins and Metalloporphyrins*; Smith, K. M., Ed.; Elsevier Scientific Publishing: Amsterdam, The Netherlands, 1975; Chapter 5.
(26) (a) Fleischer, E. B.; Srivastava, T. S. *J. Am. Chem. Soc.* **1969**, *91*, 2403. (b) Hoffman, A. B.; Collins, D. M.; Day, V. W.; Fleischer, E. B.; Srivastava, T. S.; Hoard, J. L. *J. Am. Chem. Soc.* **1972**, *94*, 3620.
(27) Stolzenberg, A. M.; Strauss, S. H.; Holm, R. H. *J. Am. Chem. Soc.* **1981**, *103*, 4763.

Table 1. Crystallographic Details for the Four Structures

	[Fe(T*p*-OCH_3PP)(2-MeHIm)]	[Fe(T*p*-OCH_3PP)(1,2-Me_2Im)]	[Fe(TPP)(1,2-Me_2Im)]	[Fe(TTP)(2-MeHIm)]
formula	$C_{52}H_{42}FeN_6O_4 \cdot 2.3C_6H_5Cl \cdot 0.2C_4H_6N_2$	$C_{53}H_{44}FeN_6O_4 \cdot C_6H_5Cl \cdot 0.5C_6H_{14}$	$C_{49}H_{36}FeN_6 \cdot C_7H_8$	$C_{52}H_{42}FeN_6 \cdot C_6H_5Cl \cdot 0.5C_6H_{14}$
FW	1146.05	1032.91	856.82	962.40
a, Å	16.2258(6)	9.7135(11)	13.0504(8)	13.9178(3)
b, Å	17.1365(7)	10.7474(13)	9.4303(6)	22.8372(4)
c, Å	20.7837(8)	25.525(3)	35.931(2)	15.4107(3)
α		85.980(2)		
β, deg	104.053(1)	87.730(2)	98.468(1)	96.999(1)
γ		74.323(3)		
V, Å^3	5606.0(4)	2558.6(5)	4373.8(5)	4861.7(2)
Z	4	2	4	4
space group	$P2_1/n$	$P\bar{1}$	$P2_1/n$	$P2_1/c$
D_c, g/cm^3	1.358	1.341	1.301	1.315
F(000)	2385	1081	1792	2020
μ, mm^{-1}	0.436	0.403	0.391	0.413
crystal dimens, mm^3	0.3 × 0.3 × 0.2	0.20 × 0.12 × 0.03	0.5 × 0.4 × 0.2	0.41 × 0.15 × 0.14
absorption correction		SADABS		
radiation, Mo Kα, $\bar{\lambda}$		0.71073 Å		
T, K	130(2)	100(2)	100(2)	100(2)
total data collected	61136	23820	47270	66800
unique data	13917 (R_{int} = 0.043)	10478 (R_{int} = 0.088)	10903 (R_{int} = 0.023)	17880 (R_{int} = 0.035)
unique obsd data [$I > 2\sigma(I)$]	10323	4470	9879	12349
refinement method		on F^2 (SHELXL)		
final *R* indices [$I > 2\sigma(I)$]	R_1 = 0.0496, wR_2 = 0.1258	R_1 = 0.0668, wR_2 = 0.1346	R_1 = 0.0396, wR_2 = 0.1077	R_1 = 0.0488, wR_2 = 0.1283
final *R* indices [for all data]	R_1 = 0.0714, wR_2 = 0.1416	R_1 = 0.1643, wR_2 = 0.1622	R_1 = 0.0434, wR_2 = 0.1123	R_1 = 0.0815, wR_2 = 0.1454

in inert oil, mounted on a glass pin, and transferred to the cold gas stream of the diffractometer. Crystal data were collected at 100 K (in case of [Fe(TPP)(1,2-Me_2Im)], [Fe(TTP)(2-MeHIm)], and [Fe(T*p*-OCH_3PP)(1,2-Me_2Im)]) or 130 K (in case of [Fe(T*p*-OCH_3PP)(2-MeHIm)]). The structures were solved by direct methods using SHELXS-97[28] and refined against F^2 using SHELXL-97;[29,30] subsequent difference Fourier syntheses led to the location of most of the remaining non-hydrogen atoms. For the structure refinement all data were used including negative intensities. All non-hydrogen atoms were refined anisotropically if not remarked otherwise below. Hydrogen atoms were idealized with the standard SHELXL-97 idealization methods. The program SADABS[31] was applied for the absorption correction. Brief crystallographic details are given for each structure in Table 1. Complete crystallographic details, atomic coordinates, anisotropic thermal parameters, and fixed hydrogen atom coordinates are given in the Supporting Information for all four structures.

[Fe(T*p*-OCH_3PP)(2-MeHIm)]·2.3C_6H_5Cl·0.2$C_4H_6N_2$. A dark-purple crystal with the dimensions 0.3 × 0.3 × 0.2 mm^3 was used for the structure determination. The 2-methylimidazole was found to be disordered over two positions, a major and a minor position. The anisotropic displacement parameters of the atoms of the minor 2-methylimidazole N(5b), N(6b), C(4b), and C(3b) were each constrained to be equal to the anisotropic displacement parameters of the corresponding atoms N(5a), N(6a), C(4a), and C(3a) of the major imidazole orientation. After the final refinement the occupancy of the major imidazole orientation was found to be 85%. The unit cell contains two fully occupied chlorobenzene molecules. A third solvent molecule (30% chlorobenzene and 20% 2-methylimidazole) was found to be disordered around an inversion center. It was refined as two rigid groups, the non-hydrogen atoms were isotropically refined. The hydrogen atoms of the major imidazole ligand were located directly from a difference Fourier and subsequently idealized while allowing the torsion angles to refine.

[Fe(T*p*-OCH_3PP)(1,2-Me_2Im)]·C_6H_5Cl·0.5C_6H_{14}. A dark-purple crystal with the dimensions 0.20 × 0.12 × 0.03 mm^3 was used for the structure determination. The axial ligand was found to have a single orientation. The asymmetric unit contains one porphyrin complex, one-half of a hexane molecule and two half molecules of chlorobenzene. Both of the chlorobenzene half molecules were found to be disordered over two positions related by an inversion center. The first chlorobenzene molecule and Cl(3S) of the second one were refined anisotropically; other atoms of the second chlorobenzene molecule and hexane molecule were refined isotropically. The chlorobenzene half-molecules were refined with the carbon atoms fixed as idealized six-membered rings that were allowed to ride on their respective chlorine atoms. One of the methoxyphenyl groups (C42···C47) had large temperature factors and was found to be disordered over two positions. However, these positions are too close to be refined independently. For hydrogen atoms of methyl C(4) and C(5), a difference electron density synthesis was calculated around the circle which represents the loci of possible hydrogen positions (for a fixed C−H distance and X−C−H angle). The maximum electron density (in the case of a methyl group after local 3-fold averaging) was taken as the starting hydrogen position. Then the hydrogen coordinates were re-idealized and rode on the atoms to which they were attached with fixed thermal parameters (u_{ij} = 1.5U_{ij}(eq)). Other hydrogen atoms were placed at idealized positions, and a riding model (u_{ij} = 1.2U_{ij}(eq)) was used for subsequent refinements.

[Fe(TPP)(1,2-Me_2Im)]·C_7H_8. A dark-purple crystal with the dimensions 0.5 × 0.4 × 0.2 mm^3 was used for the structure determination. The 1,2-dimethylimidazole was found to be disordered over two positions, a major and a minor position. The anisotropic displacement parameters of the atoms of the minor 1,2-dimethylimidazole N(5b), N(6b), C(5b), C(4b), and C(3b) were each constrained to be equal to the anisotropic displacement parameters of the corresponding atoms N(5a), N(6a), C(5a), C(4a), and C(3a) of the major imidazole ligand. After the final refinement the occupancy of the major imidazole ligand was found to be 71%. The unit cell contains one fully occupied toluene molecule. It was refined as a rigid group, the non-hydrogen atoms were

(28) Sheldrick, G. M. *Acta Crystallogr.* **1990**, *A46*, 467.
(29) Sheldrick, G. M. Program for the Refinement of Crystal Structures. Universität Göttingen, Germany, 1997.
(30) $R_1 = \sum||F_o| - |F_c||/\sum|F_o|$ and $wR_2 = \{\sum[w(F_o^2 - F_c^2)^2]/\sum[wF_o^4]\}^{1/2}$. The conventional *R*-factors R_1 are based on *F*, with *F* set to zero for negative F^2. The criterion of $F^2 > 2\sigma(F^2)$ was used only for calculating R_1. *R*-factors based on F^2 (wR_2) are statistically about twice as large as those based on *F*, and *R*-factors based on ALL data will be even larger.
(31) Sheldrick, G. M. Program for Empirical Absorption Correction of Area Detector Data; Universität Göttingen, Germany, 1996.

Scheme 1

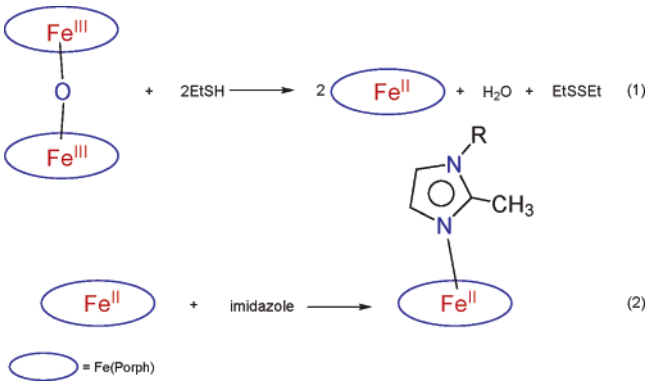

isotropically refined. The hydrogen atoms of the major imidazole ligand were located directly by using a difference Fourier and subsequently idealized while allowing the torsion angles to refine.

[Fe(TTP)(2-MeHIm)]·C_6H_5Cl·0.5C_6H_{14}. A red crystal with the dimensions 0.41 × 0.15 × 0.14 mm^3 was used for the structure determination. The asymmetric unit contains one porphyrin complex and one fully occupied chlorobenzene molecule and a half molecule of hexane. The chlorobenzene molecule is disordered over two positions and was refined as a rigid group. For the methyl hydrogen atoms of the imidazole group, a difference electron density synthesis was calculated around the circle which represents the loci of possible hydrogen positions (for a fixed C−H distance and X−C−H angle). The maximum electron density (in the case of a methyl group after local 3-fold averaging) was taken as the starting hydrogen position. Then the hydrogen coordinates were re-idealized and rode on the atoms to which they were attached with fixed thermal parameters ($u_{ij} = 1.5U_{ij}$ (eq)).

Results

The five-coordinate, imidazole-ligated, iron(II) porphyrin complexes were synthesized starting from the corresponding iron(III) μ-oxo derivatives ([Fe(Porph)]$_2$O). Ethane thiol reduction to give the iron(II) species [Fe(Porph)] was followed by reaction with a hindered imidazole ligand as shown in Scheme 1. The iron(II) species, especially four-coordinate [Fe(Porph)], are air sensitive and must be handled under rigorous inert-atmosphere conditions. Crystalline samples suitable for X-ray structure determinations were obtained by liquid diffusion of a nonsolvent layered above the porphyrin solution in sealed glass tubes. The structures of four derivatives have been obtained: [Fe(T*p*-OCH_3PP)(2-MeHIm)], [Fe(T*p*-OCH_3PP)(1,2-Me_2Im)], [Fe(TPP)(1,2-Me_2Im)], and [Fe(TTP)(2-MeHIm)]. Although two of the structures have disordered imidazole ligands, the second orientation of the imidazole has only a minor occupation, and the major orientation of the ligand dominates the structural features of the molecule.

An ORTEP diagram of [Fe(T*p*-OCH_3PP)(2-MeHIm)] is given in Figure 1. The axial ligand is disordered over two positions with a major and a minor orientation. The diagram shows the major orientation (85% occupancy) of the imidazole ligand. An ORTEP diagram showing both orientations of the axial ligand is provided in the Supporting Information (Figure S1). The labeling scheme is consistent with all of the diagrams and tables. The two orientations of the imidazole ligand are essentially coplanar; the dihedral angle between the two axial ligand planes is 0.7°. The dihedral angle (ϕ) between the major imidazole ligand and the plane defined by N(1), Fe, N(5a) is 44.7°. The

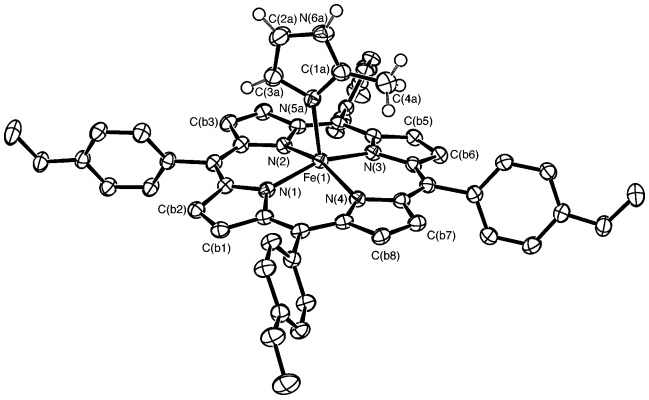

Figure 1. ORTEP diagram of [Fe(T*p*-OCH_3PP)(2-MeHIm)]. The major orientation (85%) of the imidazole ligand is shown. The hydrogen atoms of the porphyrin ligand have been omitted for clarity; the hydrogen atoms of the imidazole ligand are shown; 50 probability ellipsoids are depicted.

dihedral angle between the major imidazole ligand and the 24-atom mean porphyrin plane is 81.4°. Other selected geometric parameters involving the iron and imidazole ligand are given in Table 2 for this and the remaining structures.

[Fe(T*p*-OCH_3PP)(1,2-Me_2Im)] is illustrated in the ORTEP diagram of Figure 2. The 1,2-dimethylimidazole ligand has a single orientation. The orientation of the hydrogen atoms on the hindering methyl, as defined by the X-ray diffraction result, is illustrated in this figure. Similar orientations are seen for all of the other structures as well. The dihedral angle ϕ between the imidazole plane and the plane defined by N(4), Fe, N(5) is 20.7°. The dihedral angle between the imidazole ligand and the 24-atom mean porphyrin plane is 88.6°.

An ORTEP diagram of [Fe(TPP)(1,2-Me_2Im)] is given in Figure 3. The 1,2-dimethylimidazole ligand is disordered over two positions with the major orientation (71% occupancy) shown. The dihedral angle between the two axial ligand planes is 2.6°. The dihedral angle ϕ between the imidazole plane and the plane defined by N(1), Fe, N(5a) is 20.9°. The dihedral angle between the major imidazole ligand and the 24-atom mean porphyrin plane is 84.6°. An ORTEP diagram showing both orientations of the axial ligand is provided in the Supporting Information (Figure S2).

The final structure is that of [Fe(TTP)(2-MeHIm)] which is illustrated in Figure 4. The dihedral angle ϕ between the imidazole plane and the plane defined by N(1), Fe, N(5) is 35.8°. The dihedral angle between the imidazole ligand and the 24-atom mean porphyrin plane is 88.7°.

Illustrated in Figure 5 are formal diagrams of the porphyrin cores of the four new iron(II) imidazole structures. Given are the displacements of each atom from the mean plane of the 24-atom porphyrin core in units of 0.1 Å. The orientation of the imidazole ligand with respect to the core atoms are shown by the line with the circle representing the methyl group bound at the 2-carbon atom position. An analogous diagram showing atomic displacements from the mean plane of the four nitrogen atoms is given in the Supporting Information (Figure S3).

Also included on the diagrams of Figure 5 are the individual Fe−N_p bond lengths. The average Fe−N_p bond lengths are 2.087(7) Å for [Fe(T*p*-OCH_3PP)(2-MeHIm)], 2.076(8) Å for [Fe(T*p*-OCH_3PP)(1,2-Me_2Im)], 2.079(8) Å for [Fe(TPP)(1,2-Me_2Im)], and 2.076(3) Å in [Fe(TTP)(2-MeHIm)]. Other selected bond distances and angles are given in Table 2. A

Table 2. Selected Bond Distances (Å) and Angles (deg) for [Fe(Porph)(Im)] and Related Species[a]

complex[b]	Fe–N_p[c,d]	Fe–N_{im}[d]	ΔN_4[d,e]	Δ[d,f]	Ct···N[d]	Fe–N–C[g,h]	Fe–N–C[g,i]	θ[g,j]	ϕ[g,k]	ref
				iron(II)						
[Fe(TPP)(1,2-Me_2Im)]	2.079(8)	2.158(2)[l]	0.36	0.42	2.048	129.3(2)	124.9(2)	11.4	20.9	tw
[Fe(TTP)(2-MeHIm)]	2.076(3)	2.144(1)	0.32	0.39	2.050	132.8(1)	121.4(1)	6.6	35.8	tw
[Fe(T*p*-OCH_3PP)(2-MeHIm)]	2.087(7)	2.155(2)[l]	0.39	0.51	2.049	130.4(2)	123.4(2)	8.6	44.5	tw
[Fe(T*p*-OCH_3PP)(1,2-Me_2Im)]	2.077(6)	2.137(4)	0.35	0.38	2.046	131.9(3)	122.7(3)	6.1	20.7	tw
[Fe(TPP)(2-MeHIm)](two-fold)	2.086(8)	2.161(5)	0.42	0.55	2.044	131.4(4)	122.6(4)	10.3	6.5	9
[Fe(TPP)(2-MeHIm)]·1.5C_6H_5Cl	2.073(9)	2.127(3)[l]	0.32	0.38	2.049	131.1(2)	122.9(2)	8.3	24.0	12
average of the six	2.080(6)	2.147(13)	0.36(4)	0.44(7)	2.048(2)	131.2(10)	123.0(11)	8.6(20)		
[Fe(TpivPP)(2-MeHIm)]	2.072(6)	2.095(6)	0.40	0.43	2.033	132.1(8)	126.3(7)	9.6	22.8	11
[Fe(Piv_2C_8P)(1-MeIm)]	2.075(20)	2.13(2)	0.31	0.34	2.051	126.5	120.4	5.0	34.1	32
[Fe(TpivPP)(2-MeIm$^-$)]$^-$	2.11(2)	2.002(15)	0.52	0.65	2.045	NR[m]	NR	5.1	14.7	33
[Fe(TpivPP)Cl]$^-$	2.108(15)	2.301(2)[n]	0.53	0.59	2.040	–	–	–	–	34
[Fe(TpivPP)(O_2CCH_3)]$^-$	2.107(2)	2.034(3)[o]	0.55	0.64	2.033	–	–	–	–	35
[Fe(TpivPP)(OC_6H_5)]$^-$	2.114(2)	1.937(4)[o]	0.56	0.62	2.037	–	–	–	–	35
[Fe(TpivPP)(SC_6HF_4)]$^-$	2.076(20)	2.370(3)[p]	0.42	NR	2.033	–	–	–	–	34
[Fe(TPP)(SC_2H_5)]$^-$	2.096(4)	2.360(2)[p]	0.52	0.62	2.030	–	–	–	–	36
[Fe(TPP)(1-MeIm)$_2$][q]	1.997(4)	2.014(5)	0.0[r]	0.0[r]	1.997	128.2	128.3	1.1	14.7	37
[Fe(TPP)(THF)$_2$]	2.057(4)	2.351(3)[s]	0.0[r]	0.0[r]	2.057	–	–	–	–	38
				iron(III)						
[Fe(OEP)(2-MeHIm)]$^+$	2.038(6)	2.068(4)	0.35	0.36	2.008	131.7(3)	122.1(3)	5.0	3.9	39
[Fe(OEP)(2-MeHIm)$_2$]$^+$	2.041(11)	2.275(1)	0.0[r]	0.0[r]	2.041	134.15(10)	120.76(9)	3.2	22.2	40
[Fe(TPP)(2-MeHIm)$_2$]$^+$[q]	1.970(4)	2.012(4)	0.0	0.0	1.970	132.8	120.6	~4,4	33,32	41
[Fe(TMP)(1,2-Me_2Im)$_2$]$^+$[q]	1.937(12)	2.004(5)	0.01	0.01	1.937	134.6	119.8	NR	45,45	42
[Fe(OEP)(1-MeIm)$_2$]$^+$[q]	2.004(2)	1.975(2)	0.0[r]	0.0[r]	2.004	NR	NR	NR	20	43

[a] Estimated standard deviations are given in parentheses. [b] Unless noted otherwise, complex is high spin. [c] Averaged value. [d] In Å. [e] Displacement of iron from the mean plane of the four pyrrole nitrogen atoms. [f] Displacement of iron from the 24-atom mean plane of the porphyrin core. [g] Value in degrees. [h] 2-carbon, sometimes methyl substituted. [i] Imidazole 4-carbon. [j] Off-axis tilt (deg) of the Fe−N_{Im} bond from the normal to the porphyrin plane. [k] Dihedral angle between the plane defined by the closest N_p −Fe−N_{im} and the imidazole plane in deg. [l] Major imidazole orientation. [m] Not reported. [n] Chloride. [o] Anionic oxygen donor. [p] Thiolate. [q] Low spin. [r] Six-coordinate; required to be zero by symmetry. [s] Neutral oxygen donor.

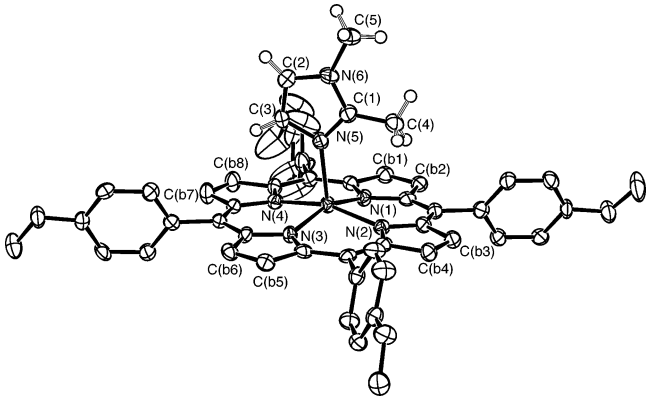

Figure 2. ORTEP diagram of [Fe(T*p*-OCH_3PP)(1,2-Me_2Im)]. The single orientation of the (ordered) imidazole ligand is shown. The hydrogen atoms of the porphyrin ligand have been omitted for clarity; 50% probability ellipsoids are depicted.

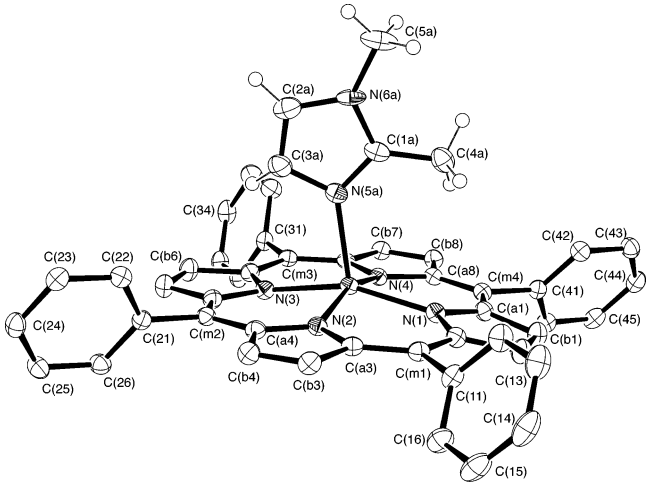

Figure 3. ORTEP diagram of [Fe(TPP)(1,2-Me_2Im)]. The major orientation of the imidazole ligand is shown. The hydrogen atoms of the porphyrin ligand have been omitted for clarity; 50% probability ellipsoids are depicted.

complete listing of bond distances and angles for all four structures is given in the Supporting Information.

The Fe−N(imidazole) bond lengths for the four structures range from 2.14 to 2.16 Å, and in all four structures the imidazole ligand Fe−N bond vector is tilted off of the normal to the 24-atom porphyrin mean plane. The value of the tilt angle, given by θ in Table 2, is 8.6° for [Fe(T*p*-OCH_3PP)(2-MeHIm)], 6.1° for [Fe(T*p*-OCH_3PP)(1,2-Me_2Im)], 11.4° for [Fe(TPP)(1,2-Me_2Im)], and 6.6° for [Fe(TTP)(2-MeHIm)]. Two other important angles associated with the imidazole ligands (Fe−N−C) are given in Table 2. The range of iron atom displacements out of the porphyrin plane is 0.38−0.51 Å. The radii of the porphyrin cores, given by Ct···N in Table 2, are nearly identical at 2.046−2.050 Å.

These crystalline species as well as others were studied with variable temperature Mössbauer spectroscopy. Both the quadrupole splitting and isomer shift values show a strong temperature dependence. The quadrupole splitting for the crystalline species [Fe(T*p*-OCH_3PP)(2-MeHIm)] at 4.2 K is 2.18 mm/s and at 298 K is 1.67 mm/s. The isomer shifts at these respective temperatures are 0.94 and 0.81 mm/s. At 4.2 K the quadrupole splitting for [Fe(T*p*-OCH_3PP)(1,2-Me_2Im)] is 2.44 mm/s and the isomer shift is 0.95 mm/s.These values at 298 K are 1.77 and 0.81 mm/s respectively. For [Fe(TPP)(1,2-Me_2Im)], ΔE_Q at 4.2K is 1.97 mm/s and δ_{Fe} is 0.92 mm/s. At 295 K these values are 1.61 and 0.82 mm/s respectively. The quadrupole splitting for the crystalline species [Fe(TTP)(2-MeHIm)] at 15 K is 2.03 and 1.40 mm/s at room temperature. The isomer shifts at these temperatures are 0.92 and 0.81 mm/s, respectively. These and the Mössbauer parameters for other iron(II)tet-

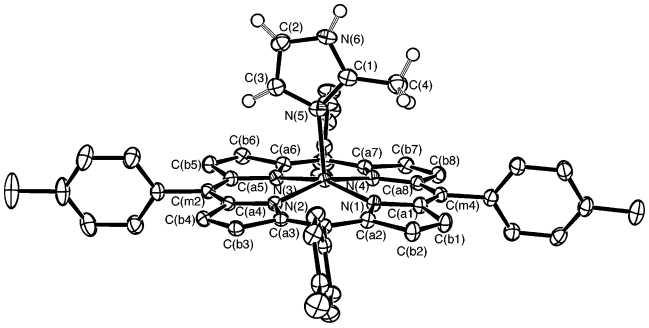

Figure 4. ORTEP diagram of [Fe(TTP)(2-MeHIm)]. The single orientation of the (ordered) imidazole ligand is shown. The hydrogen atoms of the porphyrin ligand have been omitted for clarity; 50% probability ellipsoids are depicted.

raarylporphyrins at various temperatures are given in Table S25 of the Supporting Information.

Discussion

Mössbauer /Electronic Structure. Mössbauer isomer shift (δ) and quadrupole splitting (ΔE_q) values for six new iron(II) tetraarylporphyrinates have been measured from room temperature to 4.2 K. The values of ΔE_q that were observed at 4.2 K ranged from 1.93 to 2.44 mm/s in magnitude. These are within the range of previously reported high-spin iron(II) species; the large value of the isomer shift ($\sim$0.9 mm/s) is consistent with high-spin iron(II).[44] Although the quadrupole splitting is in principle directly correlated with the detailed structure of the complex,[45] a comparison of the ΔE_q values with the respective structure does not suggest an obvious correlation.

A potential difficulty in attempting such a correlation is our observation of the appearance of polymorphic forms. The examples of [Fe(TPP)(2-MeHIm)] and [Fe(TTP)(2-MeHIm)] represent the best explored system for the issue of polymorphs. Prior to this study, the crystal system and unit cell constants for [Fe(TPP)(2-MeHIm)] had been determined for about 15 crystals for the original structural investigation[12] and subsequently for NRVS vibrational studies.[46] The oriented crystal

(32) Momenteau, M.; Scheidt, W. R.; Eigenbrot, C. W.; Reed, C. A. *J. Am. Chem. Soc.* **1988**, *110*, 1207.
(33) Mandon, D.; Ott-Woelfel, F.; Fischer, J.; Weiss, R.; Bill, E.; Trautwein, A. X. *Inorg. Chem.* **1990**, *29*, 2442.
(34) Schappacher, M.; Ricard, L.; Weiss, R.; Montiel-Montoya, R.; Gonser, U.; Bill, E.; Trautwein, A. X. *Inorg. Chim. Acta* **1983**, *78*, L9.
(35) Nasri, H.; Fischer, J.; Weiss, R.; Bill, E.; Trautwein, A. X. *J. Am. Chem. Soc.* **1987**, *109*, 2549.
(36) Caron, C.; Mitschler, A.; Riviere, G.; Schappacher, M.; Weiss, R. *J. Am. Chem. Soc.* **1979**, *101*, 7401.
(37) Steffen, W. L.; Chun, H. K.; Hoard, J. L.; Reed, C. A. *Abstracts of Papers*; 175th National Meeting of the American Chemical Society; Anaheim, CA, March, 1978; American Chemical Society: Washington, DC, 1978; INOR 15. (b) Hoard, J. L., personal communication.
(38) Reed, C. A.; Mashiko, T.; Scheidt, W. R.; Spartalian, K.; Lang, G. *J. Am. Chem. Soc.* **1980**, *102*, 2302.
(39) Scheidt, W. R.; Geiger, D. K.; Lee, Y. J.; Reed, C. A.; Lang, G. *J. Am. Chem. Soc.* **1985**, *107*, 5693.
(40) Geiger, D. K.; Lee, Y. J.; Scheidt, W. R. *J. Am. Chem. Soc.* **1984**, *106*, 6339.
(41) Scheidt, W. R.; Kirner, J. F.; Hoard, J. L.; Reed, C. A. *J. Am. Chem. Soc.* **1987**, *109*, 1963.
(42) Munro, O. Q.; Serth-Guzzo, J. A.; Turowska-Tyrk, I.; Mohanrao, K.; Shokhireva, T. Kh.; Walker, F. A.; Debrunner, P. G.; Scheidt, W. R. *J. Am. Chem. Soc.* **1999**, *121*, 11144.
(43) Mylrajan, M.; Andersson, L. A.; Sun, J.; Loehr, T. M.; Thomas, C. S.; Sullivan, E. P., Jr.; Thomson, M. A.; Long, K. M.; Anderson, O. P.; Strauss, S. H. *Inorg. Chem.* **1995**, *34*, 3953.
(44) Debrunner, P. G. In *Iron Porphyrins Part 3*; Lever, A. B. P., Gray, H. B., Eds.; VCH Publishers Inc.: New York, 1983; Chapter 2.
(45) Zhang, Y.; Mao, J.; Oldfield, E. *J. Am. Chem. Soc.* **2002**, *124*, 7829.
(46) Rai, B. K.; Durbin, S. M.; Prohofsky, E. W.; Sage, J. T.; Ellison, M. K.; Scheidt, W. R.; Sturhahn, W.; Alp, E. E. *Phys. Rev. E* **2002**, *66*, 051904−1−12.

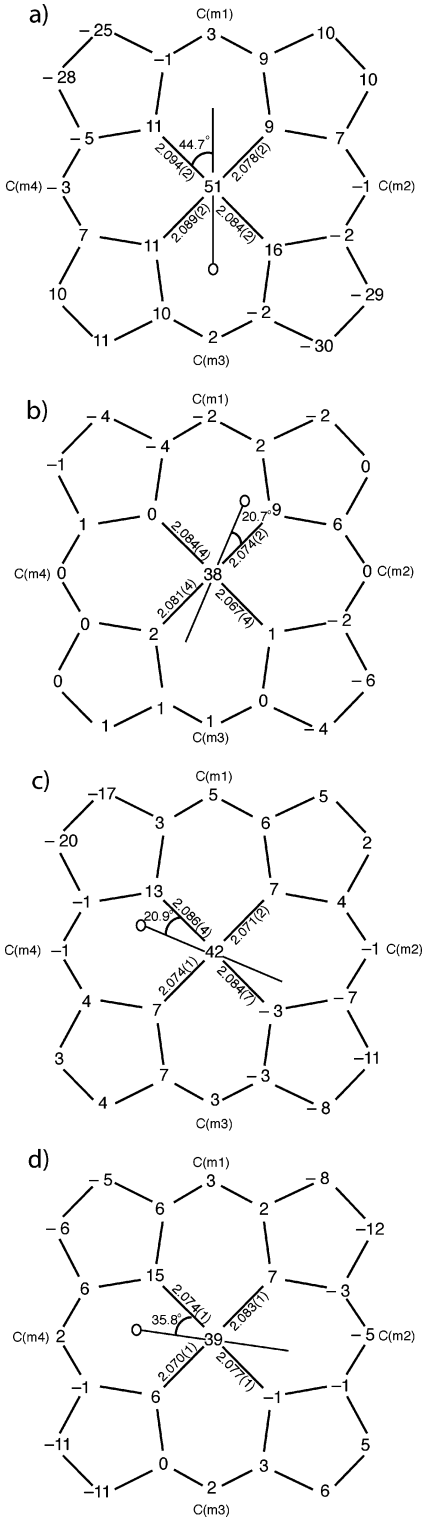

Figure 5. Formal diagrams of the porphyrinato cores of (top to bottom) (a) [Fe(T*p*-OCH_3PP)(2-MeHIm)], (b) [Fe(T*p*-OCH_3PP)(1,2-Me_2Im)], (c) [Fe(TPP)(1,2-Me_2Im)], and (d) [Fe(TTP)(2-MeHIm)]. Illustrated are the displacements of each atom from the mean plane of the 24-atom core in units of 0.01 Å. Positive values of displacement are toward the imidazole ligand. The diagrams also show the orientation of the imidazole ligand with respect to the atoms of the porphyrin core. The location of the methyl group at the 2-carbon position is represented by the circle.

NRVS studies utilized several large crystals with final specimens enriched to 95% ^{57}Fe, all crystallographically characterized and identical. These crystals were obtained from several different,

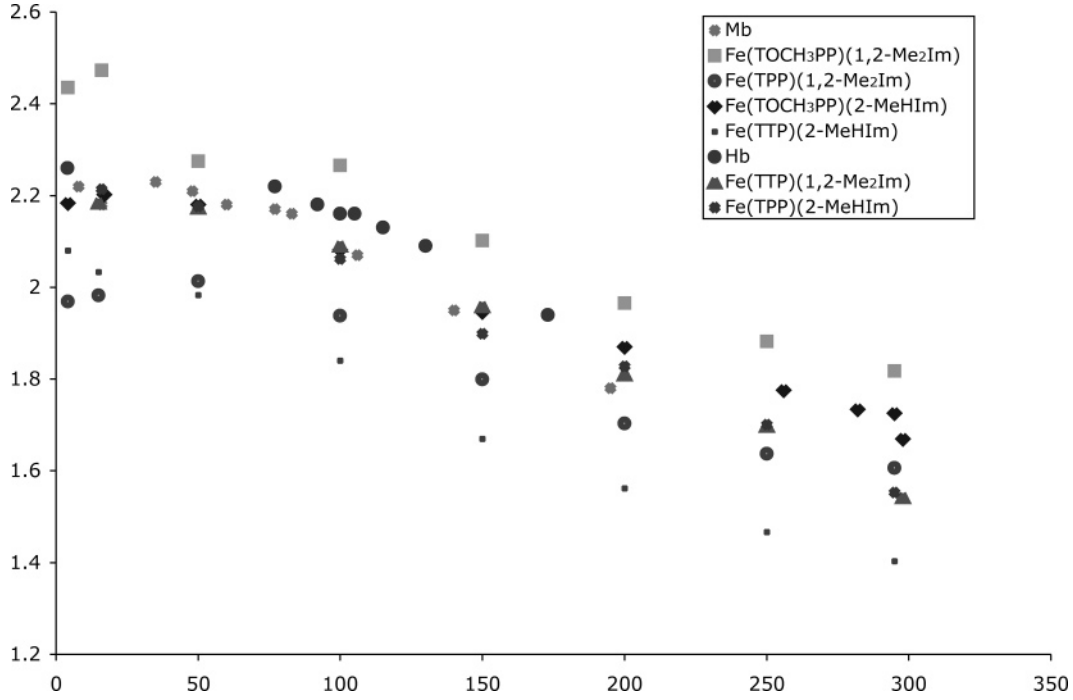

Figure 6. Plot of the temperature variation of the quadrupole splitting value as a function of temperature for the six new imidazole-ligated iron(II) porphyrinates and the heme proteins deoxymyoglobin and deoxyhemoglobin. Data for deoxymyoglobin are taken from ref 22, while those for deoxyhemoglobin are from ref 53.

independent preparations and an even larger number of crystal-growing tubes. When we subsequently made a new preparation of [Fe(TPP)(2-MeHIm)] for a complete temperature-dependent Mössbauer study, a new spectrum was obtained, not identical to that previously observed.[12] Cell constant determinations for single crystals of this new preparation revealed that a new phase had been obtained.[47] One crystal-growing tube containing an ^{57}Fe sample prepared sometime earlier was available; quite surprisingly, this sample was identical to the later sample both with respect to cell constants and Mössbauer spectrum. However, four separate preparations of the complex [Fe(TTP)(2-MeHIm)] yielded samples that had equivalent Mössbauer spectra. Limitations of experimental time did not allow such detailed comparisons on the remaining species. We did observe that two independent samples [Fe(T*p*-OCH_3PP)(1,2-Me_2Im)] were slightly different in Mössbauer values, two samples of [Fe(TPP)(2-MeHIm)] were the same, while two samples of [Fe(TTP)(1,2-Me_2Im)] were different. Complete details of all Mössbauer observations are given in Table S25.

There is a substantial temperature variation of the quadrupole splitting value; complete values of δ and ΔE_q vs T are tabulated in Table S25. A plot of the data is given in Figure 6. The value of ΔE_q decreases significantly as the temperature is increased; the temperature variation for these samples is similar over the temperature range examined. Although we have not explored the issue in detail, the maximum value of ΔE_q appears to typically be at a temperature somewhat above 4.2 K. The explanation for this temperature variation is almost certainly the presence of a number of close-lying excited states. The excited states could have the same or differing spin multiplicity relative to the ground state.

The observed temperature dependence of ΔE_q for these iron(II) tetraarylporphyrinate derivatives is similar to the variation previously seen (over a smaller temperature range) for deoxymyoglobin and -hemoglobin samples.[18,22,48−53] The observations are compared in Figure 6. It is almost certain that all of these five-coordinate imidazole-ligated species share many common features of electronic structure. A detailed study of the temperature dependence observed for deoxy-Hb was used to attempt to distinguish which of the quintet states is the ground state.[53] The ground-state thus assigned was $(d_{z^2})^1(d_{xy})^2(d_{xz})^1(d_{yz})^1(d_{x^2-y^2})^1$ with the other quintet states very close in energy. This assignment of the ground state is unlikely to be correct as is discussed below.

The application of applied magnetic field Mössbauer spectroscopy provides more rigorous information concerning the electronic ground states. Lang and co-workers pioneered in the use of applied field measurements to deoxyMb and -Hb as well as two five-coordinate model compounds, [Fe(TPP)(2-MeHIm)]-(two-fold) and [Fe(TPP)(1,2-Me_2Im)] (structure unknown). An analysis of the spectra showed the largest component of the electric field gradient, V_{zz}, to have a negative value and hence the sign of the quadrupole splitting value is also negative. For an iron compound with nonionic ligands, it is reasonable to assume that the electric field gradient (EFG) at the nucleus is dominated by contributions from the d-electrons. Given that the quadrupole splitting is negative, this clearly shows that the doubly occupied orbital must be chosen between d_{yz}, d_{xz}, or d_{z^2}, although Lang et al. did not specify which. All of the systems of Lang et al. were found to have an asymmetry parameter $\eta = (V_{xx} - V_{yy})/V_{zz} > 0.6$. As shown below, we find that the sign of

(47) Hu, C.; Scheidt, W. R. Work in progress.

(48) Kent, T. A.; Spartalian, K.; Lang, G.; Yonetani, T. *Biochim. Biophys. Acta* **1977**, *490*, 331.
(49) Bade, D.; Parak, F. *Biophys. Struct. Mechanism* **1976**, *2*, 219.
(50) Eicher, H.; Bade, D.; Parak, F. *J. Chem. Phys.* **1976**, *64*, 1446.
(51) Huynh, B. H.; Paraefthymiou, G. C.; Yen, C. S.; Wu, C. S. *J. Chem. Phys.* **1974**, *61*, 3750.
(52) Eicher, H.; Trautwein, A. *J. Chem. Phys.* **1970**, *52*, 932.
(53) Eicher, H.; Trautwein, A. *J. Chem. Phys.* **1969**, *50*, 2540.

Table 3. Mössbauer Parameters for Five-Coordinate, High-Spin Imidazole-Ligated Iron(II) Tetraarylporphyrinates and Hb and Mb

complex	ΔE_Q[a]	δ_{Fe}[a]	Γ[b]	T, K	ref
[Fe(T*p*-OCH_3PP)(1,2-Me_2Im)]	−2.44	0.95	0.46	4.2	tw[c]
[Fe(T*p*-OCH_3PP)(2-MeHIm)]	−2.18	0.94	0.58	4.2	tw
[Fe(TPP)(1,2-Me_2Im)]	−1.93	0.92	0.44	4.2	tw
[Fe(TPP)(2-MeHIm)]	−1.96	0.86	0.55	4.2	tw
[Fe(TTP)(2-MeHIm)]	−1.95	0.85	0.42	4.2	tw
[Fe(TTP)(1,2-Me_2Im)]	−2.06	0.86	0.43	4.2	tw
[Fe(TPP)(2-MeHIm)]	−2.40	0.92	0.50	4.2	12
[Fe(TPP)(2-MeHIm)(two-fold)	−2.28	0.93	0.31	4.2	22
[Fe(TPP)(1,2-Me_2Im)]	−2.16	0.92	0.25	4.2	22
[Fe((Piv_2C_8P)(1-MeIm)]	−2.3[c]	0.88	0.40	4.2	32
Hb	−2.40	0.92	0.30	4.2	22
Mb	−2.22	0.92	0.34	4.2	22
[Fe(TpivPP)(SC_2H_5)]$^-$	+2.18	0.83	0.30	4.2	57
[Fe(OC_6H_5)(TPP)]$^-$	+4.01	1.03		4.2	58
[Fe(O_2CCH_3)(TpivPP)]$^-$	+4.25	1.05	0.30	4.2	59
[Fe(OCH_3)(TpivPP)]$^-$	+3.67[d]	1.03	0.40	4.2	35
[Fe(OC_6H_5)(TpivPP)]$^-$	+3.90[d]	1.06	0.38	4.2	35
[Fe(TpivPP)(2-MeIm)]$^-$	+3.51[d]	0.97		77	33
[Fe(TpivPP)(SC_6HF_4)][$NaC_{12}H_{24}O_6$]	+2.38[d]	0.84	0.28	4.2	57
[Fe(TpivPP)(SC_6HF_4)][Na⊂222]	+2.38[d]	0.83	0.32	4.2	57
[Fe(TpivPP)Cl]$^-$	+4.36[d]	1.01	0.31	77	34

[a] mm/s. [b] Line width, fwhm. [c] Sign not determined experimentally, presumed negative. [d] Sign not determined experimentally, presumed positive.

the quadrupole splitting value for all new imidazole-ligated derivatives is also negative. Moreover, all complexes are of very low symmetry. This clearly rules out d_{z^2} as the doubly occupied orbital. The remaining pair of possible orbitals are expected to be nearly degenerate with the degeneracy lifted owing to the coordination of the planar axial imidazole ligand which will interact to differing degrees with the pair. The low symmetry deduced clearly shows a lifting of the degeneracy. We can thus conclude that the ground-state configuration for all of the imidazole-ligated iron complexes is the $(d_{xz})^2(d_{yz})^1(d_{xy})^1(d_{z^2})^1$-$(d_{x^2-y^2})^1$ configuration, and where we have chosen the d_{xz} orbital to have slightly lower energy than d_{yz}.

A similar $(d_{xz})^2(d_{yz})^1(d_{xy})^1(d_{z^2})^1(d_{x^2-y^2})^1$ ground configuration probably pertains to the six-coordinate, high-spin complex [Fe(TPP)$(THF)_2$],[54] known to have a negative quadrupole splitting (−2.75 mm/s at 4.2 K). This is consistent with the experimental X-ray electron density assignment of Lecomte et al.[55]

This newly assigned electronic configuration appears consistent with the NMR studies of Goff and LaMar on five-coordinate high-spin iron porphyrinates,[56] although they assigned the doubly occupied orbital as the d_{xy} orbital. However, this configuration ($(d_{xy})^2$) must lead to a positive sign for the quadrupole splitting value. Interestingly, there are a number of five-coordinate high-spin iron(II) porphyrinate derivatives definitely known[57−59] to have a positive value of the quadrupole splitting, while a number of others must be regarded as highly probable. These derivatives are listed in Table 3 with a "+" sign. As shown in the table, all of these complexes have an anionic species as the axial ligand.

(54) (a) Reed, C. A.; Mashiko, T.; Scheidt, W. R.; Spartalian, K.; Lang, G. *J. Am. Chem. Soc.* **1980**, *102*, 2302. (b) Boso, B.; Lang, G.; Reed, C. A. *J. Chem. Phys.* **1983**, *78*, 2561.
(55) Lecomte, C.; Blessing, R. H.; Coppens, P.; Tabard, A. *J. Am. Chem. Soc.* **1986**, *108*, 6942.
(56) Goff, H.; La Mar, G. N. *J. Am. Chem. Soc.* **1977**, *99*, 6599.
(57) Schappacher, M.; Ricard, L.; Fisher, J.; Weiss, R.; Montiel-Montoya, R.; Bill, E. *Inorg. Chem.* **1989**, *28*, 4639.
(58) Shaevitz, B. A.; Lang, G.; Reed, C. A. *Inorg. Chem.* **1988**, *27*, 4607.
(59) Bominaar, E. L.; Ding, X.; Gismelseed, A.; Bill, E.; Winkler, H.; Trautwein A. X.; Nasri, H.; Fisher, J.; Weiss, R. *Inorg. Chem.* **1992**, *31*, 1845.

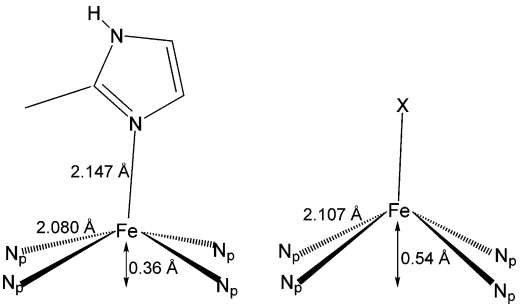

Figure 7. Comparison of the typical stereochemical features of the imidazole-ligated high-spin iron(II) complexes with a $(d_{xz})^2$ ground configuration with the anionic high-spin iron(II) complexes with a $(d_{xy})^2$ ground configuration. Data were taken from Table 2.

Thus, high-spin iron(II) porphyrinates can be divided into two different electronic configurations, those with a doubly occupied d_{xz} orbital and those with a doubly occupied d_{xy} orbital. As can be seen from a comparison of structural data (Table 2) with the signed quadrupole derivatives of Table 3, this division into two groups is also manifested in the structures. The complexes with known $(d_{xz})^1(d_{yz})^1(d_{xy})^2(d_{z^2})^1(d_{x^2-y^2})^1$ configuration have significantly larger iron atom displacements (∼ 0.18 Å larger) and equatorial Fe−N_p bonds (∼ 0.04 Å longer). To date, only the oxygen-carrying hemoproteins and their model complexes are known to have the $(d_{xz})^2(d_{yz})^1(d_{xy})^1(d_{z^2})^1(d_{x^2-y^2})^1$ configuration. It is interesting to speculate that the electronic configuration differences are related to functional or ligand binding dynamical differences. The structural differences in the two electron configuration types is schematically shown in Figure 7.

The sign of the quadrupole splitting has thus yielded, with high probability, the assignment that the ground electronic configuration is $(d_{xz})^2(d_{yz})^1(d_{xy})^1(d_{z^2})^1(d_{x^2-y^2})^1$. However, other features of the spectral analysis and the fits in magnetic field by Lang et al.[18] were regarded as being much less definitive. A particularly surprising feature was that the Mössbauer spectral analysis led to a zero-field splitting constant (D) of -5.0 cm^{-1} in the fit for the complex [Fe(TPP)(2-MeHIm)](two-fold), while on the other hand, the value of D in deoxy-Mb was a positive 4.8 cm^{-1}. This positive value was based on both the Mössbauer and magnetic susceptibility measurements. Spectra for the other model complex, [Fe(TPP)(1,2-Me_2Im)], were not fit in detail, but also suggest a negative value of D. Moreover, the value of D for deoxy-Hb was positive. This difference in the sign of D between the protein samples and the model compounds was unexpected since all show strong similarities in the Mössbauer at ambient and near-ambient temperatures. In our subsequent analysis of the magnetic Mössbauer spectrum of the second crystalline form of [Fe(TPP)(2-MeHIm)],[12] we have also found a negative value for the quadrupole splitting and a negative value of D, continuing the unanticipated distinction between the proteins and the model compounds.

What is the significance of the sign of D for these species? A difference in sign would appear to imply differences in the d-orbital energy levels of the complexes in question. The sign issue can be approached by the spin Hamiltonian approximation. The spin Hamiltonian approximation attempts to describe the ground electronic state of the systems, which for high-spin ferrous is an orbital singlet and a spin quintet, in terms of

equivalent spin operators, commonly written as[60]

$$H = D\left[S_z^2 - \frac{1}{3}S(S+1)\right] + E(S_x^2 - S_y^2) + \mu_B \vec{H}\cdot\tilde{g}\cdot\vec{S}. \quad (1)$$

The first two terms (zero-field splitting) describe the shifts in energy among the spin states due to spin/orbit coupling mixing in excited spin/orbital states, while the third term describes the Zeeman interaction between the electron spin and orbital magnetic moments and an external applied field *H*.

This Hamiltonian will only accurately describe the ground state if the energies of the excited states are large relative to the spin orbit coupling which mixes them into the ground state. The spin orbit coupling parameter λ is normally assumed to be about 100 cm^{-1} for high-spin ferrous iron. If we assume that the doubly occupied d-orbital is a d_{xz} state, then second-order perturbation theory gives the following expressions for the parameters *D* and *E*:

$$D = \frac{3}{2}\lambda^2\left[\frac{1}{3E_{xy}} + \frac{1}{3E_{x^2-y^2}} + \frac{1}{E_{z^2}} - \frac{2}{3E_{yz}}\right] \quad (2)$$

$$E = \frac{1}{2}\lambda^2\left[\frac{3}{E_{z^2}} + \frac{1}{E_{x^2-y^2}} - \frac{1}{E_{xy}}\right] \quad (3)$$

where E_{ii} is the energy of the relevant d orbital. Again, these equations assume (i) large splittings to excited states, (ii) no configurations of lower spin multiplicity have low enough energy to mix in, and (iii) one can ignore possible equivalent spin operators of fourth power in the quadratic form above (eq 1).

Since the d_{z^2} and $d_{x^2-y^2}$ orbitals are high enough in energy to be negligible, eq 2 simplifies to the following inequality for $D > 0$:

$$E_{yz} > 2E_{xy} \quad (4)$$

Equation 4 clearly shows that the sign of *D* depends on the relative energies of the excited d_{yz} and d_{xy} orbitals. A reasonable assumption would be that the energy of the d_{xy} orbital is well above that of the d_{yz} orbital given that d_{xz} is expected to be the ground state. It is thus apparent that one should expect all of the imidazole-ligated complexes to have a negative value of *D*.

We have measured the Mössbauer spectra in applied magnetic field, typically at 3, 6, and 9 T, to further examine the nature of these deoxymyoglobin and -hemoglobin models. The Mössbauer data were fit using the spin Hamiltonian model used previously by us[12] and by Kent et al.:[22]

$$H = D\left[S_z^2 - \frac{1}{3}S(S+1)\right] + E(S_x^2 - S_y^2) + \vec{H}\cdot\tilde{g}\cdot\vec{S} + H^Q - g_N^*\beta_N\vec{H}\cdot\vec{I} + \vec{S}\cdot\tilde{A}^*\cdot\vec{I} \quad (5)$$

where *D* and *E* are again the axial and rhombic zero-field splitting parameters, $\tilde{A}^*$ is the magnetic hyperfine tensor and H^Q gives the nuclear quadrupole interaction:

$$H^Q = \frac{eQV_{zz}}{12}\left[3I_z^2 - I(I+1) + \eta(I_x^2 - I_y^2)\right] \quad (6)$$

Q is the quadrupole moment of the ^{57}Fe nucleus and η is given by the components (V_{ii}) of the electric field gradient. Simultaneous fits to spectra at all fields were obtained by least-squares minimization using a downhill simplex method.[61]

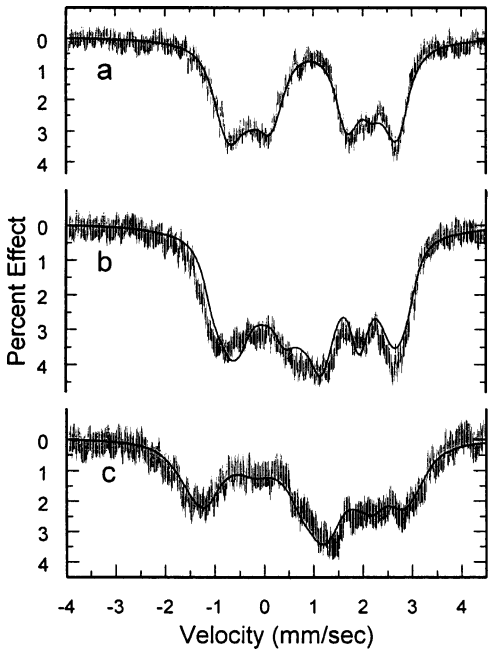

Figure 8. Figure illustrating the fits to the Mössbauer data obtained at 9 T. Spectrum (a) is that obtained for [Fe(T*p*-OCH_3PP)(1,2-Me_2Im)], spectrum (b) for [Fe(TPP)(1,2-Me_2Im)], and spectrum (c) is for [Fe(TTP)(1,2-Me_2Im)].

To obtain the best simultaneous fits to the applied-field spectra at 3, 6 and 9 T, we had to allow a nonaxial magnetic hyperfine tensor ($A_{xx}^* \neq A_{yy}^*$) and also allow the principal axes of the quadrupole tensor to rotate with respect to the axes of the *g* and $\tilde{A}^*$ tensors. The parameters that were varied for the simultaneous fits were *D*, *E*, the components of $\tilde{A}^*$, η, and the Euler angles relating the principal axes of the quadrupole and *D* tensors. Fits to the applied field Mössbauer data were obtained for the six new complexes (top six complexes of Table 3). The sign of *D* for four complexes, [Fe(T*p*-OCH_3PP)(2-MeHIm)], [Fe(TTP)(2-MeHIm)], [Fe(TPP)(2-MeHIm)], and [Fe(TTP)(1,2-Me_2Im)], were clearly found to be positive in the fitting procedure, similar to the earlier results for deoxymyoglobin and deoxyhemoglobin. Even when the fits were constrained so that $D < 0$, the *E* values so obtained were found to be defined in an improper coordinate system. Transforming *E* back to a proper coordinate system always led to the condition that *D* was positive. The sign determinations of *D* for [Fe(TPP)(1,2-Me_2Im)] and [Fe(T*p*-OCH_3PP)(2-MeHIm)] were found to be ambiguous, presumably because the magnetic splitting in applied magnetic field is small and thus not sensitive to *D*. A reexamination of the data previously obtained for one form of [Fe(TPP)(2-MeHIm)][12] still gave fits that *D* was negative.

Typical fits of the Mössbauer data in applied field for the six new derivatives are shown in Figures S4−S9 of the Supporting Information. Figure 8 shows the 9-T data for (a) [Fe(T*p*-OCH_3PP)(1,2-Me_2Im)], (b) [Fe(TPP)(1,2-Me_2Im)], and (c) [Fe(TTP)(1,2-Me_2Im)]. The significantly differing and increasing magnetic splittings are clear in the progression. It is

(60) Abragam A.; Bleaney, B. *Electron Paramagnetic Resonance of Transition Ions*; Oxford University Press: Oxford 1970.

(61) Press, W. H.; Teukolsky, S. A.; Vetterling, W. T.; Flannery, B. P. *Numerical Recipes in C, The Art of Scientific Computing*, 2nd ed.; Cambridge University Press: 1992; p 408.

to be emphasized that we required simultaneous fits to the data obtained at three different applied fields, 3, 6, and 9 T. The simultaneous fitting of spectra in 3, 6, and 9 T applied field did not completely constrain all of the parameters used in the fit. We found that adequate simulation of the observed spectra required rotation of the principal axes of the quadrupole tensor, and thus three more parameters than the minimal model of eq 5. However, for a wide range of choices of the axial ZFS parameter D the fitting algorithm was able to readjust the other parameters and achieve equally good χ-squared values for the fits. Thus, although we can be confident of the sign of D based on the requirement that D and E from the fits correspond to a proper coordinate system, we are unable to claim the determination of specific values of D for these samples. At best we can say the χ-squared had a broad minimum for D in the range of 5 cm^{-1} to as large as 30 cm^{-1}.

There are some aspects of the fit using the spin Hamiltonian (eq 1) that should be noted. First, the anisotropic part of the magnetic hyperfine tensor A should be proportional to the D tensor. If one assumes a reasonable value for the spin/orbit coupling parameter ($\lambda \approx -100$ cm^{-1}), the calculated values for D and E from the fit components of the A tensor are too large by factors as large as 3. Calculated D and E values can be adjusted to match the fit values only with a very small λ (-30 to -50 cm^{-1}), less than half of what is normally used for the free-ion value. This is an indication of strong delocalization, as λ should also be roughly proportional to the expectation value of $\langle r^{-3} \rangle$, assuming the d electrons feel an effective potential proportional to $1/r$. Second, the isotropic component of the A tensor, which measures the Fermi contact contribution to the magnetic hyperfine interaction, is quite small for most of the fits. As this component is also proportional to the expectation value $\langle r^{-3} \rangle$, this is again consistent with strong delocalization of the d-wave functions. Finally, to get acceptable χ-squared values for the fits to high-field data, we found it necessary to allow the orientation of the EFG tensor to be rotated relative to the D and A tensors. This indicates that the effective symmetry at the iron site is even lower than the rhombic symmetry assumed in eq 1.

While the spin Hamiltonian approximation (eq 5) led to acceptable fits to the magnetic Mössbauer spectra of the models for fields up to 9 T, the positive sign of D inferred from the fits is at odds with the negative sign of the quadrupole splitting, to the extent they are both explainable by a crystal field model with an isolated ground orbital. Given that λ seems to be quite small for these models, and that D (proportional to λ^2/Δ, where Δ is an excited-state energy) is likely not to be exceptionally small, we conclude that there must be low-lying excited states which mix strongly with the ground d_{xz} orbital. We note that this conclusion is also supported by the strong temperature dependence of the quadrupole splitting.

In summary, we can obtain good simultaneous fits to the field dependence of the Mössbauer spectra for these models, but the spin Hamiltonian parameters resulting are not consistent with a simple crystal field model, and lead us to doubt the applicability of the spin-Hamiltonian approximation. Proper modeling of the iron state would thus require a larger crystal field model which takes the excited states into account directly, rather than through perturbation theory. The inadequacy of the spin Hamiltonian treatment appears to be true for most, if not all, five-coordinate, imidazole-ligated, high-spin species that have been studied to date by either Mössbauer or by integer-spin EPR.

Further insight into this problem might be gained through Mössbauer data taken in higher fields than 9 T. It is possible that complete understanding of the Mössbauer results would require careful application of a crystal field model which includes all five of the d orbitals and low-symmetry crystal field potentials. Importantly, we do find among the model compounds examples that agree with the results on deoxyhemoglobin and deoxymyoglobin in having a positive sign for D.

Given the clear complexity of the electronic state of these imidazole-ligated iron(II) species, the difficulties of the theoretical calculations[14−17] in predicting the observed quintet ground state is explicable. The low symmetry of the electronic state that we infer strongly suggests that further theoretical calculations should not use any symmetry simplifications in the calculations.

Structural Results. Another goal of this study was to further investigate the structural details of the five-coordinate deoxyheme model compounds [Fe(Porph)(Im)]. There are a number of overall structural features expected for such high-spin iron(II) complexes.[62] These include an expanded porphinato core, large equatorial Fe−N_p bond distances and a significant out-of-plane displacement of the iron(II) atom. Such features were observed in a recently characterized, new crystalline form of [Fe(TPP)(2-MeHIm)][12] and an earlier, partly described crystalline form.[9] However, we found distinctly different structural features between these two nominally equivalent species. In the newer crystalline form we observed a previously unrecognized porphyrin core distortion that we ascribed to steric interaction between the axial 2-methylimidazole ligand and the porphyrin core. An even more interesting response to the steric effects of the axial ligand was found in the unsymmetrical Fe−N_p bond lengths where two short bonds result from the porphyrin ring tilting down and two long bonds result from the up-wave of the core. This is clearly illustrated in the formal diagram of the porphyrin core given in ref 12. This was in distinct contrast to the strongly domed features of the first crystalline form of [Fe(TPP)(2-MeHIm)] that also apparently led to a larger out-of-plane displacement of the iron (0.55 Å vs 0.38 Å from the 24-atom plane).

Because we thought that the structural differences between these two derivatives might relate to functional significance, we have prepared and structurally characterized several additional examples in order to determine what structural pattern, if any, is dominant. We have again employed the sterically hindered imidazole ligand strategy to make four new five-coordinate, high-spin species [Fe(Porph)(RIm)], with either 2-methylimidazole or 1,2-dimethylimidazole. The steric interaction of the methyl group with the porphyrin core when using the ligands 2-methylimidazole and 1,2-dimethylimidazole greatly reduces K_2 without significantly affecting K_1.[63] All of the porphyrin derivatives were meso-substituted tetraarylporphyrins.

A summary of the structural parameters for the four new examples is given as the first four entries of Table 2. Although disorder in the position of the axial imidazole ligand has been considered a major problem for this class of derivative, two of

(62) Scheidt, W. R.; Reed, C. A. *Chem. Rev.* **1981**, *81*, 543.
(63) Rougee, M.; Brault, D. *Biochem. Biophys. Res. Commun.* **1974**, *57*, 654.

the derivatives have a single, ordered axial ligand and the other two have a major orientation of the ligand. As expected, the general structural features that are common to five-coordinate iron(II) high-spin species are seen for these four structures. These include an expanded porphyrin core where Ct···N is 2.05 Å, long equatorial Fe−N_p bond lengths where the averages range from 2.076(3) Å to 2.087(7) Å, and moderately large iron atom out-of-plane displacements (ΔN_4 > 0.32 Å). In addition, the large size of the iron(II) ion has been thought to lead to a significant C_{4v} doming of the core. A measure of the doming is given by the difference between the displacement of the iron atom from the mean plane of the four nitrogen atoms (ΔN_4) and the mean plane of the 24-atom core (Δ). Also listed in Table 2 are the values previously reported for the two forms of [Fe(TPP)(2-MeHIm)].[9,12] Averaged values for these six derivatives are given on the next line. Values for other species are also given in Table 2 for further discussion.

There are several necessary structural responses to binding a hindered imidazole to form the five-coordinate iron porphyrinates. The overall effect required is to maximize the attractive interaction between iron and its ligands while minimizing the repulsive interaction between the 2-methyl group of the imidazole ligand and the porphyrin plane. This is accomplished by adjustments in the tilting of the Fe−N(Im) bond off of the normal to the heme plane, the Fe−N(Im)−C(Im) angles, the iron out-of-plane displacement, the Fe−N(Im) bond length, and the orientation of imidazole plane with respect to the porphyrin core. However, there is still considerable variation among these geometric parameters.

Although these structural features are a result of the large size of the high-spin iron(II) ion and the asymmetric steric bulk of the axial ligand, an examination of the values in Table 2 shows that there is significant variation within the set of six imidazole-ligated high-spin five-coordinate iron(II) derivatives. While the radius of the central hole (Ct···N) remains constant at 2.048(2) Å, the value of the average Fe−N_p bond distances in the complexes varies from 2.073 Å up to 2.087 Å. The displacement of the iron atom from the four nitrogen atom mean plane shows a range of 0.32 to 0.42 Å while the iron displacement from the 24-atom plane shows a larger range of variation; the difference between the two displacements shows a still larger variation. The difference in displacement between the two planes range from as low as 0.03 Å ([Fe(T*p*-OCH_3-PP)(1,2-Me_2Im)]) to 0.13 Å ([Fe(TPP)(2-MeHIm)](two-fold)). To understand these variations we first examine the atomic displacements of the four new derivatives from the 24-atom mean plane. This information is given in Figure 5. The core conformation of the four derivatives are clearly very different. They range from a "domed" conformation for [Fe(T*p*-OCH_3-PP)(2-MeHIm)] to a "tented" conformation for [Fe(TTP)(2-MeHIm)] to one pyrrole ring showing large displacement from the mean plane ([Fe(TPP)(1,2-Me_2Im)]) to a close-to-planar conformation for [Fe(T*p*-OCH_3PP)(1,2-Me_2Im)]. The orientation of the imidazole ligands are also shown in Figure 5; there is no apparent correlation between the core conformation and the ligand orientation.

The four new derivatives have different core conformations, but there are some similarities to the core conformations previously observed for *both* crystalline forms of [Fe(TPP)(2-MeHIm)]. Core conformations of the six tetraarylporphyrin

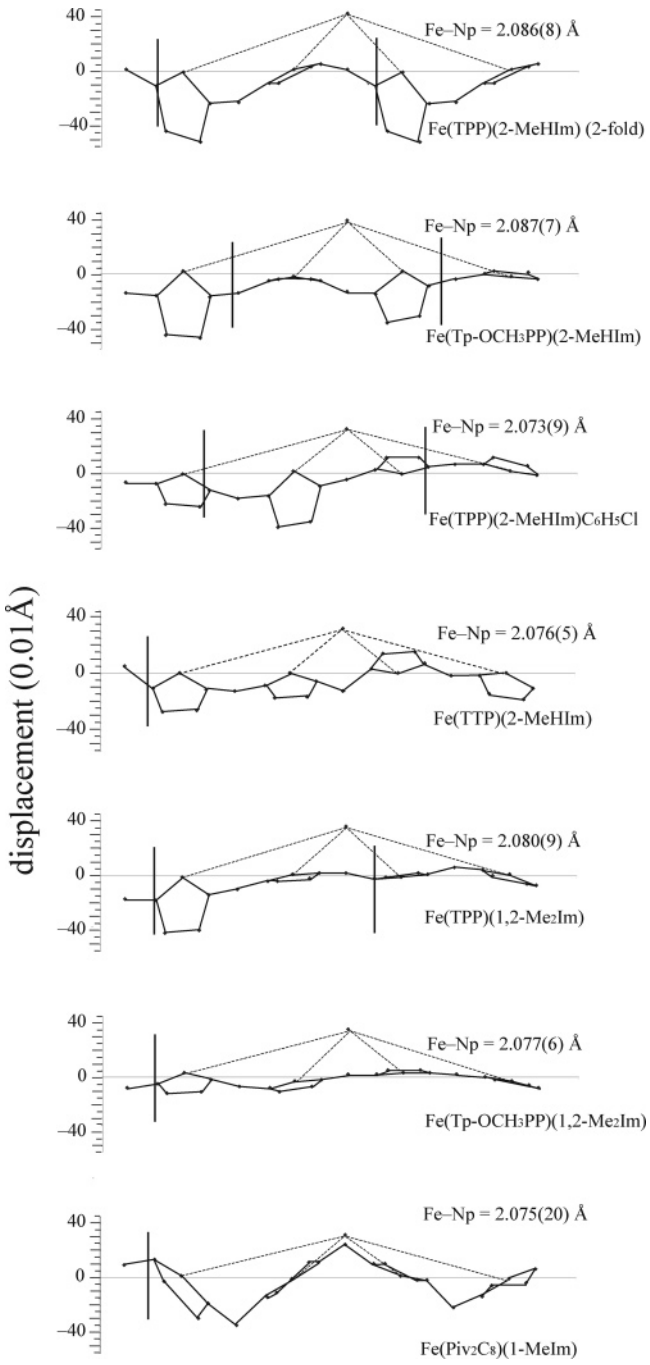

Figure 9. Diagrams illustrating the core conformation and iron displacement for seven known imidazole-ligated high-spin iron(II) porphyrinates. The displacement of the iron and the atoms of the porphyrin core from the mean plane defined by the four pyrrole nitrogen atoms is given. The position of the imidazole ligand with respect to directions defined by the Fe−N_p directions is shown.

derivatives along with a hybrid porphyrin system are illustrated in Figure 9. Displayed in linear fashion are the displacements of the iron atom and the 24 atoms of the porphyrin core from the four pyrrole nitrogen atom mean plane. The structures are illustrated with the derivative having the largest displacements of the atoms from the plane at the top and then in the order of decreasing displacements; the hybrid porphyrin structure is shown last. The orientation of the imidazole ligand with respect to the porphyrin core is also shown: the vertical line represents the position of the imidazole shown with the pyrrole closest to

the 2-methyl group. When there is a minor orientation this is illustrated with a second vertical line; the major orientation is always shown to the left. With the exception of the [Fe(TPP)(2-MeHIm)](two-fold) structure, which has two equivalent orientations of the axial ligand, it is expected that the major ligand orientation dominates the observed structure.

The strong similarity in the core conformations between the "domed" conformation of [Fe(TPP)(2-MeHIm)](two-fold)[9] and that of [Fe(T*p*-OCH_3PP)(2-MeHIm)] is clearly seen in the top two structures illustrated in Figure 9. These two structures have a number of similarities in addition to core conformation. The iron displacements from the N_4 and 24-atom planes are the largest for these two derivatives (0.42 and 0.55 Å for [Fe(TPP)(2-MeHIm)](two-fold), and 0.39 and 0.51 Å for [Fe(T*p*-OCH_3-PP)(2-MeHIm)]). Concomitant with the large displacement of the iron, the average Fe−N_p distances (2.086 and 2.087 Å) are also the largest for these two derivatives.

The core conformations of the second form of [Fe(TPP)(2-MeHIm)] and [Fe(TTP)(2-MeHIm)] also display similarities as can be seen from the third and fourth entries of Figure 9. The unusual feature first noted in [Fe(TPP)(2-MeHIm)][12] that the core conformation asymmetry apparently induced by the axial ligand leads to unequal Fe−N_p bond distances is also seen in the tetratolyl derivative. The Fe−N_p bond distances appear to fall into two distinct categories. In both derivatives, the two pyrrole rings that bracket the 2-methyl group are tilted downward. The Fe−N_p bonds to these two pyrrole rings appear to be shortened while the opposite two are lengthened. The pattern of distances can be seen in Figure 5d. In Fe(TPP)(2-MeHIm)] the two pairs have values of 2.066(4) and 2.081(3) Å, a statistically significant difference, whereas the pair values of 2.072(3) and 2.080(4) Å in [Fe(TTP)(2-MeHIm)] are somewhat less significant. These two derivatives have the smallest iron atom displacements from the N_4 plane (0.32 Å) and very modest amounts of core doming. The overall effect of these various conformational features lead to overall average Fe−N_p bond distances that are shorter than those seen for the domed conformers.

The last two new compounds, both 1,2-dimethylimidazole derivatives, have porphyrin cores that have only one pyrrole ring that is significantly tilted from the N_4 mean plane with the remaining three rings nearly exactly planar. These are displayed as the fifth and sixth compounds in Figure 9. The tilted pyrrole ring is, not unexpectedly, the ring closest to the bulky methyl group of the imidazole. The magnitude of the iron displacement from the N_4 plane has increased slightly from those of the previous set (average ΔN_4 value 0.35 Å).

The final derivative illustrated in Figure 9 is the only known five-coordinate high-spin iron(II) derivative with an unhindered imidazole ligand.[32] To achieve this, a hybrid porphyrin with both a strap and two pickets, all on one side of the porphyrin plane, must be used to allow access to only one face of the porphyrin. This is the only known high-spin iron(II) complex with a strongly ruffled core. It is most likely that the trans superstructure strap leads to the core ruffling. Although the N_4 and 24-atom planes are nearly coincident and core ruffling usually leads to shortened M−N_p bonds, the iron atom displacement and Fe−N_p distances appear to be unaffected and are not outside the range of the other derivatives described herein.

The results summarized in Figure 9 make evident that there is not a *single* preferred conformation for imidazole-ligated high-spin iron(II) complexes. Although doming of the porphyrin core, which leads to a substantial displacement of the iron from the N_4 plane and a larger displacement from the 24-atom plane, might be expected to best accommodate the large high-spin iron(II) center, a number of other conformations are also observed. Variations in core conformations and iron atom displacement notwithstanding, all derivatives have porphyrin cores in which the radial expansion of the central hole is effectively constant at 2.048 Å. These variations do lead a modest range of Fe−N_p bond distances from 2.073 to 2.087 Å. The low electronic symmetry and close-lying states of iron may be reflected in the high variability of the core conformations.

The ORTEP drawings of Figures 1-4 clearly show that the axial Fe−N_{Im} bond vector is tilted from the heme normal. The tilt angle ranges from 6.1 to 11.4°. This tilting is the partial result of minimizing the interaction between the bulky imidazole methyl group and the porphyrin core; unequal Fe−N−C angles in the imidazole also serve to minimize the steric interactions. As seen in Table 2, these angles have an average value of 131.2° on the methyl side and 123.0° on the other side. However, these structural features are also seen in [Fe(Piv_2C_8P)(1-MeIm)], albeit with smaller values, suggesting that the steric interactions are not the sole factor in the asymmetric binding of the imidazole ligand. The small differences in ligand tilting appears not to be correlated with any other structural feature, showing no apparent relation to varying core conformation or the orientation of the axial ligand plane with respect to Fe−N_p directions.

The Fe−N(imidazole) bond lengths for the four structures show a small but significant variation. The small variation is no doubt an accommodation to the hindering methyl group and differences in relative orientation of the axial ligand and differing core conformations. All Fe−N(imidazole) values are nominally longer than the one value for an unhindered imidazole bound to an iron(II) ([Fe(Piv_2C_8P)(1-MeIm)]), but the differences are statistically not significant. The rather short distance observed in [Fe(TpivPP)(2-MeHIm)] may be artifactual; the rigid group refinement parameters used to describe the disordered imidazole had an unusually small C−N−C angle.

Summary. The extensive Mössbauer studies undertaken in this investigation clearly show that all imidazole-ligated high-spin iron(II) porphyrinates have a negative value for the quadrupole splitting and the most likely ground electronic configuration of all is the $(d_{xz})^2(d_{yz})^1(d_{xy})^1(d_{z^2})^1(d_{x^2-y^2})^1$ configuration. Although we failed to achieved absolute conclusions concerning the sign of the zero-field splitting constant *D*, we have shown that an apparent dichotomy in the sign between the model compounds and the heme protein systems is illusory. The electronic state of all these derivatives is of extremely low symmetry. For all species there are close-lying excited states of unknown spin multiplicity. High-spin iron(II) porphyrinates can be divided into two classes of electronic configuration with significantly different geometric structures. The importance of these features for heme protein functionality remains unknown but intriguing. The structural characterization of four deoxyhemoglobin models has been reported. All derivatives have an iron atom displacement of ∼0.36 Å from the four nitrogen atom plane with larger displacements and larger variation in displacement from the 24-atom plane reflecting core conformation

differences. Although there are a number of differing core conformations observed, there are some strong similarities with all falling into perhaps three classes of conformation.

Acknowledgment. We thank the National Institutes of Health for support of this research under Grant GM-38401. We thank Dr. Bruce Noll and A. Beatty for assistance with X-ray data collection.

Supporting Information Available: Tables S1−S24, giving complete crystallographic details, atomic coordinates, bond distances and angles, anisotropic temperature factors, and fixed hydrogen atom positions for all four structures; Table S25, giving complete values of Mössbauer quadrupole splitting and isomer shift as a function of temperature; Table S26 giving the derived crystal field parameters obtained; Figure S1 showing the two disordered axial imidazoles in [Fe(T*p*-OCH_3PP)(2-MeHIm)]; Figure S2 giving the same information for [Fe(TPP)-(1,2-Me_2Im)]; Figure S3 showing the displacement of the core atoms from the four nitrogen atom plane; Figures S4−S9 giving illustrations of the Mössbauer spectra and fits in 3-, 6-, and 9-T applied magnetic field for [Fe(TPP)(2-MeHIm)], [Fe(TPP)-(1,2-Me_2Im)], [Fe(TTP)(2-MeHIm)], [Fe(TTP)(1,2-Me_2Im)], [Fe(T*p*-OCH_3PP)(2-MeHIm)], and [Fe(T*p*-OCH_3PP)(1,2-Me_2-Im)], respectively (PDF). An X-ray crystallographic file, in CIF format, is available. This material is available free of charge via the Internet at http://pubs.acs.org.

JA044077P